PHYSICAL REVIEW B VOLUME 51, NUMBER 14 1 APRIL 1995-II

Two-dimensional vortex and phase fluctuations from current-voltage characteristics of $Bi_2Sr_2CaCu_2O_{8+x}$ films with various oxygen contents

G. Balestrino, A. Crisan,* D. V. Livanov,† E. Milani, and M. Montuori
Dipartimento di Ingegneria Meccanica, Università di Roma–Tor Vergata,
Via della Ricerca Scientifica e Tecnologica, I-00133 Roma, Italy

A. A. Varlamov†
Forum: Institute for Condensed Matter Theory, Istituto Nazionale di Fisica della Materia,
Pisa-Florence, L. E. Fermi 2, Florence, I-50125 Italy

(Received 8 November 1994)

Current-voltage characteristics of 2212-phase epitaxial $Bi_2Sr_2CaCu_2O_{8+x}$ films have been measured in a temperature region about 8 K wide immediately below T_c. It is shown that the power law $V = A\, I^a$ valid for two-dimensional (2D) systems does not correctly describe the data, and interlayer coupling must be taken into account. The 2D approximation still remains valid at high currents, so that a crossover from 2D to 3D behavior is observed as the current is reduced. Furthermore, annealing treatments in redox atmospheres change the interlayer coupling, therefore leading to an increase of the critical current density and a decrease of the anisotropy factor with increasing oxygen content in the film. These effects can be quantitatively evaluated fitting the I-V curves with a theory due to Jensen and Minnhagen valid for quasi-2D systems. Not too far from T_c, however, an additional dissipation appears besides the Jensen-Minnhagen contribution in the low-voltage region. We propose to explain this in terms of fluctuations of the phase of the order parameter. The calculated effect is in reasonable agreement with the experimental data. As the oxygen content in the sample is varied the relative weight of the two contributions changes in qualitative agreement with the proposed fluctuation origin of the additional dissipation at low voltages.

INTRODUCTION

One of the most interesting properties of high-T_c superconducting oxides is the high anisotropy of their properties due to weak coupling among superconducting Cu-O layers. The in-plane resistivity is lower than the transversal one by a factor of about 10^2 [for $YBa_2Cu_3O_7$ (YBCO)] to 10^4 [for $Tl_2Sr_2CaCu_2O_8$ (TSCCO)].[1] Since this anisotropy affects the pinning energies and the fluxons interaction, it is of paramount importance for many superconducting properties of these materials. Because of the change of the coherence length with temperature, the anisotropy in the superconducting properties is a function of temperature, so that these systems show a crossover from two-dimensional (2D) to three-dimensional (3D) behavior when the temperature approaches the critical one.

The role of anisotropy in determining the superconducting properties of these compounds can be understood comparing the behavior of samples of a specific high-temperature superconductor having the same crystallographic and morphological quality but different degrees of anisotropy. A very simple way to obtain such samples is to change the anisotropy of superconducting oxides by varying their oxygen content by means of thermal treatments in reducing or oxidizing atmospheres. Actually, an increase in oxygen concentration leads to a stronger coupling between Cu-O planes in these systems.[2] Also, a change in oxygen concentration alters the carrier (hole) density.[3] The combination of these two effects gives rise to a number of interesting phenomena.

In particular, in $Bi_2Sr_2CaCu_2O_{8+x}$ (2212 BSCCO) an increase in the oxygen content leads to an increase of both the carriers concentration and the Cu-O planes coupling, leading to an increase of the critical current density J_c and a decrease of both the resistivity and the transition temperature T_c, while the opposite effects are observed when the oxygen content is decreased, until a maximum value of T_c (about 94 K) is reached, after which further reduction again decreases T_c.[4] On the other hand, the critical temperature of YBCO monothonically increases with oxygen stoichiometry up to a maximum value of about 93 K. The thermoelectric power vs temperature curves are shifted towards lower values as the oxygen content is increased.[5]

The c-axis resistivity is also affected by oxygen concentration. In fact, the transverse resistivity as a function of temperature shows a peak close to T_c which can be explained by means of thermal fluctuations[6,7] and is strongly dependent on the interlayer coupling and carrier density, and therefore on the oxygen stoichiometry. It turns out that this peak is very pronounced in highly anisotropic samples (BSCCO annealed in reducing atmosphere) but almost absent in samples with low anisotropy (YBCO, BSCCO annealed in oxygen atmosphere).[7–9]

The change in the anisotropy factor $\gamma = (\rho_c/\rho_{ab})^{1/2}$

(ρ_c,ρ_{ab} are the transverse and in-plane resistivities, respectively) induced by redox thermal treatments has been inferred from the shape of the resistivity transition of a BSCCO film close to T_c, and a decrease of more than one order of magnitude of γ was found from the reduced to the oxidized state.[10]

The dissipation in the absence of magnetic field close to the zero-resistance critical temperature can be described in terms of current-induced breaking of thermally activated vortex-antivortex pairs. Since vortex-antivortex interaction is influenced by the interplanar coupling the detailed shape of the resistivity transition and of the current-voltage characteristics close to T_c also depend on the oxygen stoichiometry. For strictly 2D systems the Kosterlitz-Thouless model[11] can be applied, leading to a power-law dependence of voltage as a function of current $V = AI^{\alpha}$, where α is a temperature-dependent coefficient abruptly changing from 3 to 1 at the Kosterlitz-Thouless transition temperature T_{KT}. The above formula implies the absence of any critical current, since dissipation is present at all currents. Clearly, for real systems, even if highly anisotropic as BSCCO, this picture must be modified to take into account the interplanar coupling. This has been done by Jensen and Minnhagen[12] who calculated the energy of vortex-antivortex pairs in a stack of Josephson coupled superconducting layers and derived the current-voltage formula $V \pm AI[(I/I_c)-1]^{a-1}$, which correctly implies the existence of a critical current I_c below which no voltage appears. As it was found[13] this formula correctly describes the behavior of YBCO films. For the more anisotropic BSCCO, *I-V* curves of single crystals have been recently measured[14] and fitted with the 2D power law $V = AI^{\alpha}$. However, close inspection of the data reported in Ref. 14 shows that this fit is good only in a temperature range of about 2 K below T_c, while for lower temperatures a deviation from the 2D behavior is apparent in the low current region, suggesting that even for BSCCO the strictly 2D approach is not correct.

In this paper we study the current-voltage (*I-V*) characteristics of BSCCO films at different temperatures ranging from T_c to about 8 K below T_c. These curves are analyzed in the framework of the Jensen-Minnhagen (hereafter JM) theory. A good fit with the experimental data is obtained far enough from T_c (but in the temperature range mentioned above). In the vicinity of T_c a deviation from the JM law is found in the low-voltage region and we explain it in terms of superconducting order-parameter phase fluctuations. In the immediate vicinity of T_c, that is for temperatures above the Kosterlitz-Thouless critical temperature T_{KT}, the resistive behavior of the *I-V* characteristics takes place due to the vortex-antivortex spontaneous dissociation and this effect is dominant. The effects of oxygen stoichiometry on the *I-V* curves are also discussed in the framework of the above-mentioned dissipation mechanisms.

EXPERIMENTAL DETAILS

The *I-V* curves measurements have been performed on 2212 BSCCO films grown on $NdGaO_3$ substrates by liquid-phase epitaxy (LPE). This technique has been shown to produce high quality, truly epitaxial BSCCO films when a substrate having a good in-plane lattice match with BSCCO is used. A detailed description of the growth procedure and of the structural and transport characterization of BSCCO films grown by LPE can be found elsewhere.[15,16] The zero-resistance critical temperature T_{c0} (defined as the temperature at which the resistivity drops below the measurement resolution, corresponding to less than 10^{-5} of its room-temperature value) was $T_{c0} = 79.5$ K for the as-grown film, while the room-temperature resistivity was about 2.5×10^{-4} Ω cm. A bias current of 50 μA, corresponding to 25 A/cm^2 was used to obtain resistivity data. The mosaic spread of the film, measured with an x-ray diffractometer on the intense (00 10) Bragg reflection, is 0.10^0, and the film thickness, measured with a SEM microscope, is about 2000 Å.

The *I-V* curves were measured using the standard four-probe technique on a stripe about 1 mm wide and 7 mm long patterned on the film. Contacts were made with silver paste and annealed in air at 500 °C for 1 h; the same contacts were used throughout all measurements to avoid influence of small inhomogeneities in the sample. For each curve more than 50 points were taken, while the sample was kept at a temperature (measured by a calibrated GaAs diode) stable within about ±0.02 K. A delay was introduced between each current pulse and the following one to minimize heating effects in the sample: the length of the delay time was adjusted to ensure that *I-V* curves were retraced when the current was decreased from the maximum value down to zero (i.e., no time hysteresis was observed in the curves). For each point measurements were taken for both current flow directions, and the results were averaged to compensate for thermoelectrical effects.

The oxidizing thermal treatments were carried out at a temperature of 500 °C for 1 h in oxygen atmosphere and followed by slow cooling to room temperature in the same atmosphere, while reducing ones were made at a temperature of 550 °C (again for 1 h) in argon atmosphere and followed by quenching. The effects of these thermal treatments were checked to be fully reversible.

RESULTS AND DISCUSSION

A. Survey of results

Figure 1 shows the resistance vs temperature curves for our BSCCO film in the three oxidation states: as-grown, reduced, and oxidized. All curves show a metallic behavior at high temperatures, followed by a sharp transition to the superconducting state. As expected[17] the oxidizing treatment leads to a reduction of both the resistivity and T_c with respect to the as-grown values, while the opposite is true for the reducing annealing, so that the three curves intersect each other. The transition width is not significantly affected by oxygen stoichiometry.

In Fig. 2 the *I-V* characteristics for the as-grown sample are shown at several temperatures ranging from 72 K (about 8 K below T_{c0}) to 79.5 K (T_{c0}). An additional

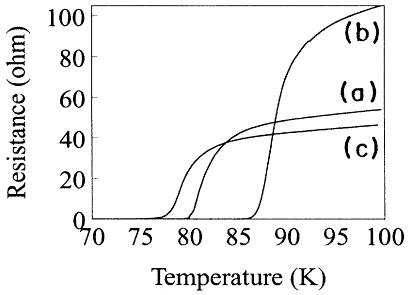

FIG. 1. Resistance vs temperature curves of the BSCCO film in different oxidation states: (a) as-grown, (b) argon annealed, (c) oxygen annealed.

curve was measured at $T=75.55$ K but is not reported in Fig. 2 to avoid superposition with neighboring curves. It is clear that the *I-V* characteristics are not straight lines in a log-log scale, as required by the power law $V=AI^{\alpha}$ valid for strictly two-dimensional systems.[2] They exhibit a downward curvature in the high-voltage region suggesting a truly superconducting behavior with vanishing linear resistance. On the other hand in the low-voltage region, not too far from T_c, an additional contribution to dissipation appears, unforeseen in the JM theory. It is worth mentioning that a similar contribution has been observed by other authors.[18,19] Similar curves were measured on the same sample after reduction (in the temperature range from 74 to 85.5 K, T_{c0} being 86 K) and oxidation (in the temperature range from 65 to 73.5 K, $T_{c0}=75$ K). The overall appearance of these curves is similar to those plotted in Fig. 2 for the as-grown sample.

B. Jensen-Minnhagen behavior

The failure of the 2D power-law formula $V \propto I^{\alpha}$ is clearly due to the fact that the coupling between superconducting layers has been neglected in the original Kosterliz-Thouless approach. Jensen and Minnhagen[12] took into account this coupling and, under the assumption that the dissipation mechanism is current-induced vortex pair breaking in a quasi-two-dimensional system, derived the formula

$$V=AI\left[\frac{I}{I_c}-1\right]^{a-1}, \tag{1}$$

which is valid for temperatures not very close to T_c (when fluctuations of the order parameter can be neglected and the superconductor is certainly below T_{KT}), and which correctly predicts the existence of a finite critical current I_c. When $I \gg I_c$ this formula reduces to the 2D one. In fact as the current is increased the in-plane vortex-antivortex interaction becomes stronger with respect to interplane one, so that in the high current region the 2D picture is expected to be applicable.

As the input current is decreased a crossover is therefore expected from a 2D to a quasi-2D behavior, appearing as a change in the slope of the *I-V* curves plotted in a log-log scale. For high currents (voltages higher than about 1 mV, not shown in Fig. 2) for *I-V* curves can indeed be fitted with the 2D power law with good results, showing a change in the slope $\alpha(T)$ as a function of temperature at $\alpha \cong 3$, which is a characteristic feature of the Kosterlitz-Thouless transition.[20] If, however, the full voltage region shown in Fig. 2 is considered, the power-law fit is clearly not satisfactory, while a good fit is obtained for temperatures not very close to T_c by the formula

$$\ln V=\ln\left[AI\left[\frac{I}{I_c}-1\right]^{a-1}\right], \tag{2}$$

which derives from the JM formula (1). The logarithms have been taken to give proper weight to the low-voltage data.

The results of the fit are shown in Fig. 3 for the as-grown film. The fit is of the same quality for the reduced and oxidized samples, not reported in Fig. 3. From the fit the values of the three fitting parameters A, I_c (and therefore J_c, the critical current density) and $a-1$ can be ex-

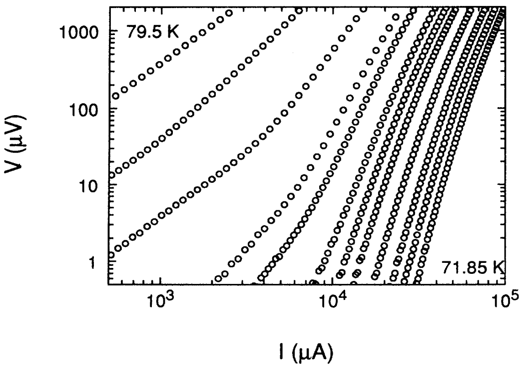

FIG. 2. *I-V* characteristics of the as-grown film at temperatures 71.85, 72.89, 73.81, 74.93, 75.91, 76.45, 76.94, 77.61, 77.92, 78.51, 79.07, and 79.50 K.

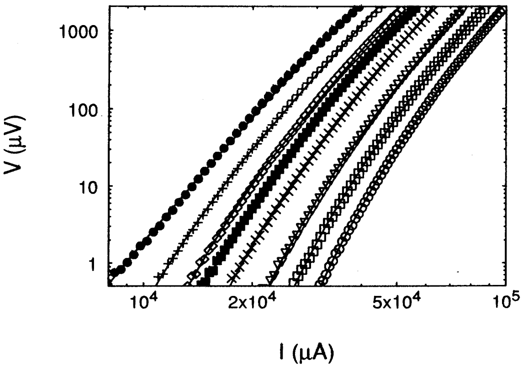

FIG. 3. *I-V* characteristics of the as-grown BSCCO film at various temperatures: (○)=71.85 K, (□) =72.89 K, (∇)= 73.81 K, (×) =74.93 K, (■)= 75.55 K, (◊) =75.91 K, (+) = 76.45 K, (●) = 76.94 K. Full lines represent best fits according to the Jensen-Minnhagen model.

tracted from the curves for which the fit is satisfactory (i.e., for temperatures not too close to T_{c0}). Since these parameters are functions of temperature, and the temperature scale defined by the critical temperature is different for different oxygen contents in the sample, to allow direct comparison between the data relative to the three oxidation states of the sample, we rescale all temperature dependences in terms of the reduced temperature $t=T/T_{c0}$.

Apart from the amplitude factor A, these fitting parameters are connected in a simple way to important physical properties of the superconductor.[12] The most important among them is clearly the critical current I_c, which is directly proportional to the coupling energy between layers. From Ref. 12 we see that I_c is proportional to the two-dimensional superconducting particles density and inversely proportional to the anisotropy factor γ. Therefore, J_c must increase with decreasing reduced temperature and with increasing oxygen content in the film, as it is evident from Fig. 4. In particular, for a given value $t=t^*$ of the reduced temperature the ratio between critical currents in the oxidized state and in the as-grown one is roughly 2–2.5, while that between the as-grown and the reduced state is about 5–8.

Since

$$\gamma=\frac{1}{J_c(0)}=\frac{1-t}{J_c(t)}\ , \tag{3}$$

from the data shown in Fig. 4 the ratios among the anisotropy factors in the three oxidation states of the sample can be calculated. it turns out that there is a continuous increase in the anisotropy factor as the oxygen stoichiometry is increased, and that this increase is by a factor of about 2 going from the oxidized to the as-grown sample, and by a factor of about 5 going from the as-grown to the reduced sample, depending on the reduced temperature value. The ratios of the anisotropy parameter for the oxygen annealed, as grown and argon annealed films are $\gamma_{\mathrm{ox}}:\gamma_{\mathrm{ag}}:\gamma_{\mathrm{red}}\simeq 1:2:10$, in agreement with those found[9,21] with different methods for BSCCO samples. The behavior of J_c with temperature is close to the linear relation $J_c(t)\propto(1-t)$ as expected from the JM model.

Another important issue which can be obtained from the fit is the value of the critical exponent $a-1$ in the JM formula. It also depends on the oxidation state, showing the tendency to assume higher values and to change its temperature dependence as the oxygen content is increased. The values of $T(a-1)$ are plotted against reduced temperature in Fig. 5. They show a weak temperature dependence for all samples, as it was found to be the case also for YBCO.[13] Moreover, the values of $T(a-1)$ show a tendency to increase as the oxygen content is increased. This is consistent with the theory since[12]

$$T(a-1)\sim\frac{1}{\lambda^2(0)}\sim\frac{1}{\rho_{ab}}\ ,$$

where $\lambda(0)$ is the London penetration depth, and the normal-state resistivity ρ_{ab} is shown in Fig. 1 to increase with decreasing oxygen content.

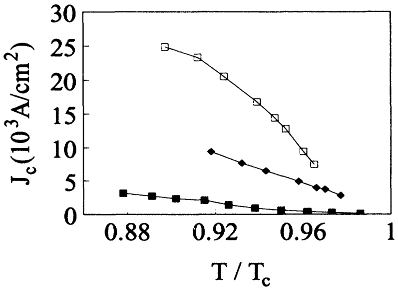

FIG. 4. Critical current density vs reduced temperature curves of the BSCCO film in different oxidation states: full rhombs = as-grown, full squares = argon annealed, open squares = oxygen annealed.

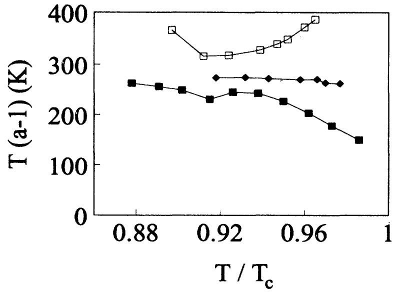

FIG. 5. Values of the critical exponent $a-1$ multiplied by temperature vs reduced temperature for the BSCCO film in different oxidation states: full rhombs = as-grown, full squares = argon annealed, open squares = oxygen annealed. Lines are only guides to the eye.

As expected, all the $T(a-1)$ values are above the lower bound $2T_{c0}$ given by the Kosterlitz-Thouless theory, with the exception of the value corresponding to $t=0.986$ for the argon-annealed sample. However, this curve is the last one which can be fitted using the JM formula alone (see following paragraph), so that a larger error is to be expected on the parameters values for this curve, due also to the very low value of J_c.

C. Order-parameter phase fluctuations

From Fig. 2 it is apparent that in the low-voltage region the I-V characteristics no more follow the JM formula, an excess dissipation appearing which changes the curvature of the characteristics. We attribute this excess dissipation to superconducting order-parameter phase fluctuations, which are not taken into account in the JM model and which become relevant at low currents when the current-induced vortex pair breaking is low.

The effect of superconducting fluctuations on I-V characteristics above T_c was studied a long time ago[22,23] and reexamined recently for layered superconductors.[24] It was shown that a nonlinear effect in fluctuation induced current manifests itself at high enough electric fields $[E>E_c=E_0\varepsilon^{3/2}$, where $\varepsilon=(T-T_c)/T_c$ and $E_0=2^{9/2}K_BT_c/\pi e\xi_{ab}(0)$, K_B is the Boltzmann constant, e the electron charge and ξ_{ab} the in-plane correlation length] and its physical origin was related to the breakdown of fluctuation Cooper pairs by strong electric fields. The power α in the excess current density $\delta J_{\rm fl} \sim E^{\alpha}$ depends on the effective dimensionality of fluctuations and a Lawrence-Doniach type crossover (2D to 3D) may take place in the I-V characteristics with α changing from 1/3 to 2/3 at temperatures close to T_c.[24] However in the case of BSCCO, whose crossover temperature is given by[8] $|(T_{\rm cr}-T_c)/T_c| \cong 7\zeta(3)w^2/32\pi^2T_c^2 \sim 0.01$ [w is the effective interlayer hopping energy and $\zeta(x)$ is the Riemann zeta function], practically for all temperatures except in the immediate vicinity of T_c the fluctuations have 2D character. In this case the results of Ref. 24 can be written for $T > T_c$ as

$$\delta J_{\rm fl}^{\rm 2D}=(e^2/16a\hbar)\begin{cases}E/\varepsilon & \text{for } E \ll E_c\\ (1/3)\Gamma(1/3)E_0(E/E_0)^{1/3} & \text{for } E \gg E_c\end{cases} \qquad (4)$$

a being the interplanar spacing and $\Gamma(x)$ the Euler gamma function.

The estimate of the critical field $E_c = E_0\varepsilon^{3/2}$ for BSCCO gives the discouragingly high value $E_c \sim 20$ V/cm ($E_0 \sim 2\times10^4$ V/cm, $\varepsilon \cong 0.01$), which can hardly be reached experimentally.[24] However this limitation is valid above T_c only, being absent in the temperature range under consideration here. To understand this we need to compare the origin of superconducting fluctuations above and below T_c. In contrast to the simple fluctuation picture in the normal phase, where nonequilibrium Cooper pairs appear and decay, the construction of a fluctuation theory below T_c based on one-particle representation implies the necessity to extend the simple BCS description of superconductivity. Really, below T_c, where the coexistence of Cooper pairs condensate and one-particle excitations in thermodynamical equilibrium takes place in BCS theory, the fluctuation processes include a variety of options: the appearance and decay of nonequilibrium (with respect to condensate) Cooper pairs, different types of quasiparticle scattering processes involving the condensate, etc. Formally, matrix elements beyond the usual $\langle N|\ldots|N\rangle$ and $\langle N|\ldots|N+2\rangle$ must be taken into account.[25]

There is another way to treat the fluctuation phenomena in the superconducting phase, that is to consider fluctuations of the amplitude and phase of the order parameter and calculate their correlations which determine the effects of fluctuations on the physically observable quantities.[25] It is worth stressing that in this scheme, in contrast to the situation above T_c, fluctuations of the scalar potential Ψ must be taken into account along with fluctuations of the phase Φ: the former determines the flow of dissipative currents, the latter is responsible for fluctuation supercurrents in the system, but they are linked and cannot be separated. This fact manifests itself formally in the appearance of a nonzero off-diagonal correlator $\langle \Phi(r,t)\Psi^*(r',t')\rangle$ and physically in a dissipation indirectly related to phase fluctuations.

Above T_c fluctuations of the modulus and phase of the order parameter are essentially equivalent and their correlators are equal[25]

$$\langle \Delta\Delta^*\rangle_{q,\omega} = \langle \Phi\Phi^*\rangle_{q,\omega} = -\frac{1}{\nu}\frac{1}{\varepsilon-(i\pi\omega/8T_c)+\eta q^2}, \qquad (5)$$

(here ν is the single-spin quasiparticle density of states, q and ω the momentum and frequency of Cooper pair, respectively, and η is the gradient coefficient in the Ginsburg-Landau theory.[25] While for zero boson frequency the propagator of amplitude fluctuations takes a form similar to Eq. (5) with the substitution of ε by $2|\varepsilon|$ only, the phase-phase correlator becomes "massless:"

$$\langle \Phi\Phi^*\rangle_{q,\omega} \sim \frac{-1}{\nu}\frac{1}{\eta q^2}. \qquad (6)$$

It is this singularity that leads to the well-known destruction of the long-range order by long-wavelength fluctuations in the case of low-dimensional electron spectrum.[26] The absence of the "mass" (whose role is played by ε) in the $\langle \Phi\Phi^*\rangle$ correlator indicates the possibility of the appearance of a Goldstone, or "soft," mode in the spectrum of collective excitations. Usually this mode is absent in superconductors at low frequencies because of the electric charge of the electron liquid,[25,27] but in the case of weak screening in the vicinity of T_c traces of it manifest themselves in the so-called Anderson-Goldman mode.[27] The absence of a "mass" ε in the phase-phase correlator means the absence of an ohmic regime in Eq. (4) because $E_c = E_0\varepsilon^{3/2} \rightarrow 0$ as $\varepsilon \rightarrow 0$.

The contribution of fluctuations of the phase of the order parameter to the excess current for any electric field is therefore given by the second line in Eq. (4), which can be rewritten as

$$E_{\rm fl} = E_0\left[\frac{48a\hbar}{e^2\Gamma(1/3)E_0}\right]^3 J^3. \qquad (7)$$

Clearly, in spite of the independence of Eq. (7) on ε (and therefore T), this contribution takes place only in the proximity of T_c, since the condition $\varepsilon \ll 1$ has been used in the above theory. Far enough from T_c the propagation of the Anderson-Goldman mode at low frequencies is impossible and the phase-fluctuation contribution disappears.

The contribution to dissipation given by Eq. (7) has a slope 3 in a $\log V$-$\log I$ plot, and is masked by the higher JM contribution at high currents. In order to test the validity of Eq. (7) we must therefore select an I-V characteristic at a temperature low enough for the JM theory to be applicable, but not so low that the phase-fluctuation contribution disappears. We have therefore chosen the curve at $T = 77.61$ K for which there is a JM behavior at voltages higher than about 10 μV, while in the low-voltage region a clear deviation from this behavior is observable, having a slope very close to 3. If we extrapolate the JM behavior valid in the high-voltage region ($V < 10$ μV), we clearly see that the JM contribution to dissipation corresponding to a current $I = 5$ mA (or lower) is negligible with respect to the measured value of slightly more than 1 μV. This value should therefore be due to

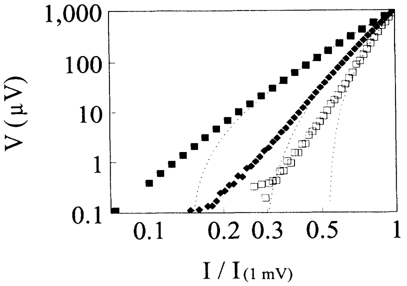

FIG. 6. *I-V* curves of the BSCCO film in different oxidation states (full rhombs = as-grown, full squares = argon annealed, open squares = oxygen annealed) at reduced temperatures 0.984, 0.986, and 0.980, respectively. Current normalized to the value corresponding to a voltage drop of 1 mV. Dashed lines are fits with the Jensen-Minnhagen model performed on the voltage region 100–1000 μV.

the contribution resulting from Eq. (7) with an electric field $E_{\text{fl}} = V/L = 1.4$ μV/cm ($L = 7$ mm is the length of the stripe). This gives (taking into account the section of the stripe $s = 2\times10^{-6}$ cm^2) $I \cong 2.5$ mA, a value in order-of-magnitude agreement with the experimental one.

The threshold at which the deviation from the JM formula is significant shifts to lower reduced temperatures for a given voltage (or to higher voltages at given reduced temperature) as the oxygen content is increased and therefore the anisotropy is decreased. In fact the fit (carried out on the experimental points for which $V > 500$ nV) ceases to be satisfactory for $t > 0.965$, $t > 0.977$, $t > 0.986$ for the oxidized, as-grown and reduced sample, respectively. This is consistent with the above proposed fluctuation origin of this contribution. In fact, Eq. (7) being temperature independent, it describes a "universal" curve having equation $V \sim I^3$ in the *I-V* plane, so that for the most oxidized samples, whose *I-V* curves are shifted, at given reduced temperatures, towards the high current region, the fluctuation contribution is higher, with respect to less oxidized samples.

To clarify this point we plotted in Fig. 6 the *I-V* curves for all three samples at very similar reduced temperatures (namely $t = 0.980$ for the oxygen annealed sample, $t = 0.984$ for the as-grown one, and $t = 0.986$ for the reduced one) in a reduced temperature region in which fluctuation effects are not negligible. The current has been normalized for all samples to the value corresponding to a voltage of 1 mV because the large spread of critical current values among the three samples makes a direct comparison impossible on the same scale. It can be seen that while the curve for the argon-annealed sample shows no visible deviation from the JM behavior, as indicted by the negative curvature, a deviation is apparent in the curve for the as-grown samples for $V > 10$ μV, while for the oxygen annealed sample the deviation appears at even larger voltages ($V > 100$ μV), even if the reduced temperature, and therefore fluctuation effects, are (however slightly) higher for the less oxygenated samples. To further prove this point a fit with the JM model has been performed on the three curves in a voltage region (100–1000 μV) where the fit is good for all three samples, and the results are shown as dashed lines in Fig. 6. The deviation of the fit from the experimental data occurs at higher voltages as the oxygen content is increased.

CONCLUSIONS

We have analyzed the *I-V* characteristics of an epitaxial BSCCO film grown by liquid-phase epitaxy at different temperatures and for different oxidation conditions. The *I-V* curves cannot be fitted with a simple 2D power law, except at high currents. The formula proposed by Jensen and Minnhagen for quasi-2D systems, which takes into account the interplanar coupling, leads to a good fit to the experimental data in the temperature region for which vortex-antivortex depairing can be thought to be the main dissipation mechanism. From the fit the critical current density can be calculated, and is found to increase with the oxygen content in the film. Also, a comparison among the anisotropy factor γ of the sample in the various oxidation states can be carried out, showing that γ increases with decreasing oxygen stoichiometry, being roughly one order of magnitude higher for the reduced sample than for the oxidized one.

Not too far from T_c, however, a deviation from the Jensen-Minnhagen behavior is evident in the low-voltage region, which we have explained in terms of fluctuations of the phase of the order parameter: the calculated effect is in reasonable quantitative agreement with the experimental data. The relative weight of the two contributions has also been examined as a function of oxygen content in the sample and found in qualitative agreement with the proposed fluctuation origin of the additional dissipation at low voltages.

ACKNOWLEDGMENTS

One of us (D.V.L.) would like to thank the cooperation program between the University of Roma-Tor Vergata and the Moscow Institute of Steel and Alloys. A.C. would like to thank Contract No. 5153 of The Commission of the European Communities.

---

*On leave of absence from the Institute of Physics and Technology of Materials, Bucarest, Romania.

†On leave of absence from the Department of Theoretical Physics, Moscow Institute of Steel and Alloys, Leninskiy pr. 4, 117936 Moscow, Russia.

[1] S. Martin, A. T. Fiory, R. M. Fleming, G. P. Espinosa, and A. S. Cooper, Appl. Phys. Lett. **54**, 72 (1989).

[2] R. Kleiner, F. Steinmeyer, G. Kunkel, and P. Mueller, Phys. Rev. Lett. **68**, 2394 (1992).

[3] D. B. Mitzi, C. W. Lombardo, A. Kapitulnik, S. S. Laderman, and R. D. Jacowitz, Phys. Rev. B **41**, 6564 (1990).

[4] G. Balestrino, M. Marinelli, E. Milani, A. Paoletti, and P.

Paroli, J. Appl. Phys. **73**, 3903 (1993).

[5]M. F. Crommie, A. Y. Liu, M. L. Cohen, and A. Zettl, Phys. Rev. B **41**, 2526 (1990).

[6]L. Ioffe, A. I. Larkin, A. A. Varlamov, and L. Yu, Phys. Rev. B **47**, 8936 (1993).

[7]G. Balestrino, M. Marinelli, E. Milani, A. A. Varlamov, and L. Yu, Phys. Rev. B **47**, 6037 (1993).

[8]G. Balestrino, E. Milani, and A. A. Varlamov, Physica C **210**, 386 (1993).

[9]C. Baraduc, V. Pagnon, A. Budzin, J. Y. Henry, and C. Ayache, Phys. Lett. A **166**, 267 (1992).

[10]G. Balestrino, D. V. Livanov, and M. Montuori, Physica C **234**, 77 (1994).

[11]J. M. Kosterlitz and D. J. Thouless, J. Phys. C **6**, 1181 (1973).

[12]H. J. Jensen and P. Minnhagen, Phys. Rev. Lett. **66**, 1630 (1991).

[13]T. Freltoft, H. J. Jensen, and P. Minnhagen, Solid State Commun. **78**, 635 (1991).

[14]A. K. Pradhan, S. J. Hazell, J. W. Hodby, C. Chen, Y. Hu, and B. M. Wanklyn, Phys. Rev. B **47**, 11 374 (1993).

[15]G. Balestrino, V. Foglietti, M. Marinelli, E. Milani, A. Paoletti, and P. Paroli, Solid State Commun. **79**, 839 (1991).

[16]G. Balestrino, M. Marinelli, E. Milani, A. Paoletti, and P. Paroli, J. Appl. Phys. **68**, 361 (1990).

[17]G. Balestrino, M. Marinelli, E. Milani, M. Montuori, A. Paoletti, and P. Paroli, J. Appl. Phys. **72**, 191 (1992).

[18]C. Dekker, R. H. Koch, B. Oh, and A. Gupta, Physica C **185-189**, 1799 (1991).

[19]P. J. King, A. Jirk, R. M. Bowly, K. Benedict, J. S. Lees, Y. Hioki, S. Iwama, C. M. Pegrum, and R. M. Bowman, Solid State Commun. **83**, 55 (1992).

[20]D. R. Nelson and J. M. Kosterlitz, Phys. Rev. Lett. **39**, 1201 (1977).

[21]G. Balestrino, D. V. Livanov, E. Milani, B. Camarota, D. Fiorani, and A. M. Testa, Phys. Rev. B **50**, 3446 (1994).

[22]J. P. Hurault, Phys. Rev. **179**, 494 (1969).

[23]L. P. Gor'kov, Sov. Phys. JETP Lett. **11**, 32 (1970).

[24]A. A. Varlamov and L. Reggiani, Phys. Rev. B **45**, 1060 (1992).

[25]A. A. Varlamov and V. Dorin, Sov. Phys. JETP **57**, 1089 (1983).

[26]P. C. Hohenberg, Phys. Rev. **158**, 383 (1967).

[27]I. O. Kulik, O. Entin-Wohlman, and R. Orbach, J. Low Temp. Phys. **43**, 591 (1981).